Anisotropy of magnetoresistivities in $Sr_4Ru_3O_{10}$: Evidence for an orbital-selective metamagnetic transition

D. Fobes,[1] T. J. Liu,[1] Z. Qu,[1] M. Zhou,[1] J. Hooper,[1] M. Salamon,[2] and Z. Q. Mao[1,*]
[1]*Department of Physics, Tulane University, New Orleans, Louisiana 70118, USA*
[2]*University of Illinois at Urbana–Champaign, Urbana, Illinois 61801, USA*
(Received 7 April 2010; published 7 May 2010)

We have investigated magnetic field orientation dependences of intraplanar and interplanar magnetoresistivity [$\rho_{ab}(B,\phi,\theta)$ and $\rho_c(B,\phi,\theta)$] for $Sr_4Ru_3O_{10}$, which exhibits a puzzling coexistence of ferromagnetism and metamagnetism. We find that $\rho_{ab}(B,\phi)$ exhibits a remarkable field-dependent ferromagnetic anisotropy below and above the metamagnetic transition field B_c while $\rho_c(B,\phi)$ displays anisotropy from spin polarization only when field is above B_c. These observations strongly support that the metamagnetic transition in $Sr_4Ru_3O_{10}$ is orbital selective.

DOI: 10.1103/PhysRevB.81.172402 PACS number(s): 75.75.−c, 72.15.Qm, 68.37.Ef, 72.25.Ba

Orbital physics in transition-metal oxides is among the central topics in the physics of strongly correlated electron systems. In these materials the orbital degree of freedom is typically active and has a complex interplay with charge, spin, and lattice degrees of freedom, resulting in a wide range of unique electronic and magnetic properties. Examples include orbital ordering in vanadium oxides,[1,2] orbital ordering and orbital-driven ferroelectricity in manganese oxides,[3,4] orbital ordering and an orbital-selective Mott transition in $Ca_{2-x}Sr_xRuO_4$,[5–8] and orbital-dependent superconductivity in Sr_2RuO_4.[9,10] In this Brief Report we will show that the magnetism in $Sr_4Ru_3O_{10}$ is governed by the orbital degree of freedom and that its metamagnetic transition is orbital selective. To our knowledge this may be the first example of an itinerant metamagnetic transition involving orbital selection.

$Sr_4Ru_3O_{10}$ is the $n=3$ member of the Ruddlesden-Popper series of strontium ruthenates $Sr_{n+1}Ru_nO_{3n+1}$ and shows puzzling magnetic properties. For field applied along the c axis it exhibits typical ferromagnetic (FM) behavior with $T_c \approx 105$ K.[11,12] However, below 50 K, moderate fields applied in the ab plane induce a metamagnetic transition.[11,12] This metamagnetic transition occurs via a phase separation process[13–15] and is accompanied by enhanced spin-phonon coupling,[16] an anomaly in specific heat,[17] and an unusual increase in thermopower.[18]

How both metamagnetism and ferromagnetism coexist within this material is not yet resolved. To reveal the underlying physics we have investigated magnetic field orientation dependencies of intraplanar and interplanar magnetoresistivity for $Sr_4Ru_3O_{10}$. Since $Sr_4Ru_3O_{10}$ has a quasi-two-dimensional structure similar to those of Sr_2RuO_4 and $Sr_3Ru_2O_7$, the interplanar resistivity (ρ_c) should reflect transport properties of charge carriers from the Ru $4d_{xz,yz}$ orbitals hybridized with apical O $2p$ orbitals, while the intraplanar resistivity (ρ_{ab}) should primarily probe charge carriers from the Ru $4d_{xy}$ orbitals hybridized with the planar O $2p$ orbitals. This premise is supported by the large ratio of ρ_c/ρ_{ab} in $Sr_4Ru_3O_{10}$ [~383 at 0.3 K (Ref. 19)]. In our experiment we combine this directional magnetotransport measurement with angle-resolved magnetoresistivity measurements, which we found very effective in extracting orbital information of the magnetic states.

Utilizing these techniques we found that ρ_{ab} and ρ_c display distinctly different anisotropic properties under in-plane magnetic fields. ρ_{ab} exhibits a remarkable field-dependent FM anisotropy with a twofold symmetry below the metamagnetic transition field B_c and a fourfold symmetry above B_c, whereas ρ_c shows a fourfold symmetry attributable to spin polarization only when the applied field is increased above B_c. In addition, we observe a giant decrease in ρ_c attributable to spin polarization when applied field is above B_c and rotated from the c axis toward the ab plane. These observations strongly suggest that the metamagnetic transition in $Sr_4Ru_3O_{10}$ is orbital selective, where the $d_{xz,yz}$ orbitals are responsible for the observed metamagnetic transition.

The crystals used in this study were grown by floating-zone technique[19] and screened by x-ray diffraction and by superconducting quantum interference device magnetization measurements to exclude intergrowth of any other layered phases with different n. Crystal orientation was determined using Laue x-ray diffraction. Our magnetoresistivity measurements were performed in a Quantum Design Physical Property Measurement System (PPMS), and a He^3 cryostat equipped with a rotating sample stage, utilizing a four-probe technique.

Our previous work revealed three distinct magnetic phases in different magnetic field ranges (applied in the ab plane),[13–15] as shown schematically in Fig. 1(a). LP represents the lowly polarized phase where FM domains are present; this phase occurs below the metamagnetic transition. FFM denotes a forced FM state with a single domain, which occurs above the metamagnetic transition. MIX stands for the mixed phase of LP and FFM through which the metamagnetic transition occurs. We observe three different anisotropies corresponding to these three magnetic phases in the azimuthal angle dependence of in-plane magnetoresistivity $\rho_{ab}(B,\phi)$ measured with $\theta \approx 90°$ [see Fig. 1(c)]. In the LP phase (<2 T) we observe twofold symmetry of the form $A+D\sin^2(\phi)$ (where A and D are constants), which breaks down as B approaches 2 T. Fitting is shown by the solid line over 1.5 T in Fig. 1(c). The amplitude of the anisotropy in magnetoresistivity [AMR, defined as $(\rho_{max}-\rho_{min})/\rho_{min}$] significantly increases with increasing field. In the mixed phase (2–3.5 T) the anisotropy changes dramatically; we observe a

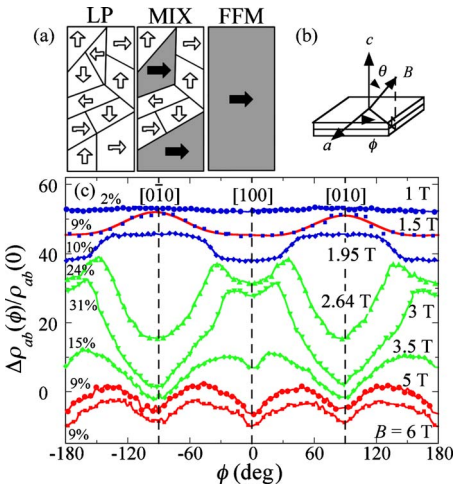

FIG. 1. (Color online) (a) Schematic representation of the three magnetic phases previously observed in $Sr_4Ru_3O_{10}$ (Refs. 13 and 14) (see text). (b) Definition of polar and azimuthal angles used in this Brief Report. ϕ=0° and θ=90° is [100] (a axis) and θ=0° is [001] (c axis). (c) Normalized azimuthal angle dependence of in-plane magnetoresistivity $\Delta\rho_{ab}(\phi)/\rho_{ab}(0)$ at selected applied magnetic fields and 2 K, where $J \| a$. From the top down, 1, 1.5, and 1.95 T are within the LP phase, 2.64, 3, and 3.5 T are within the mixed phase, and 5 and 6 T are within in the FFM phase. The solid curve at 1.5 T represents a theoretical fitting. The relative magnitude of anisotropy is indicated in percentage.

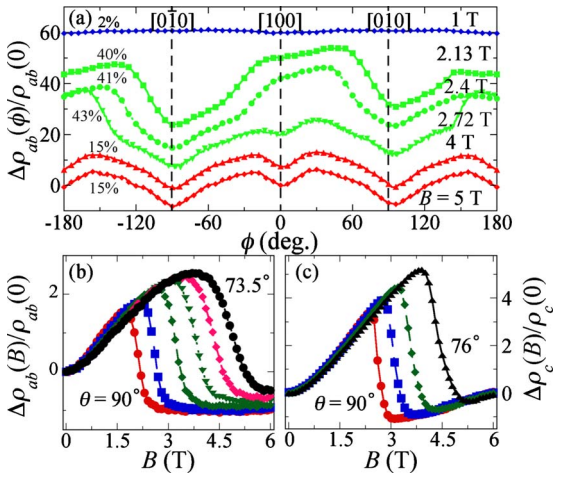

FIG. 2. (Color online) (a) Normalized azimuthal angle dependence of in-plane magnetoresistivity $\Delta\rho_{ab}(\phi)/\rho_{ab}(0)$ for a second ρ_{ab} sample at selected applied magnetic fields and 2 K. The relative magnitude of anisotropy is indicated in percentage. Field dependence of normalized magnetoresistivity at selected polar angles for (b) ρ_{ab} and (c) ρ_c at 2 K. From left to right, magnetoresistivity data were taken at θ=90, 86.5, 85.5, 83.5, 78.5, and 73.5° for ρ_{ab} and θ=90, 84, 80, and 76° for ρ_c.

large maxima centered at [100], where in the LP phase a minima was located. Additionally, a clear local minima with significantly smaller amplitude is superimposed over the large maxima at [100]. Finally, in the FFM phase (>3.5 T) we observe a fourfold symmetry with minima at [100] and [010], unique from the anisotropy seen in the LP and mixed phases.

These anisotropic properties seen in various magnetic phases are unrelated to the anisotropy which may be caused by the polar angle misalignment with $\theta \neq 90°$. To verify this we have performed a control experiment. In Fig. 2(a) we present $\rho_{ab}(B,\phi)$ data for a second sample which was intentionally misaligned with $\theta \approx 80°$. A remarkable misalignment effect on the anisotropy was only observed in the mixed phase, manifesting as an overt asymmetry of the large peak centered at [100]. This misalignment effect arises from the variation in polar angle during azimuthal rotation and the polar angle dependence of B_c [see Fig. 2(b)]. Moreover, we performed systematic measurements of field sweep of ρ_{ab} at various ϕ, $\rho_{ab}(B,\phi)$. From these measurements the maximum misalignment the sample experiences under azimuthal rotation is estimated to be $\Delta\theta_{tilt}$=2.5° for the sample presented in Fig. 1(c) (sample 1) and 8° for the sample presented in Fig. 2(a) (sample 2). For sample 1, the magnitude of anisotropy caused by misalignment is estimated to be <1% in the LP and FFM phases, and <1.5% in the mixed phase. They are all far smaller than the observed maximum AMR for these three phases (10% for LP, 9% for FFM, and 31% for MIX).

The azimuthal angle dependence of normalized interplanar magnetoresistivity, $\Delta\rho_c(\phi)/\rho_c(0)$ is shown in Fig. 3. In contrast with the FM anisotropy seen in ρ_{ab}, in the LP phase ρ_c anisotropy has a small, weakly field dependent, non-FM anisotropy with fourfold symmetry, where minima are at [100] and [010] (note: angle range in Fig. 3 is 180°, not 360° as in Fig. 1), which can be attributable to Fermi-surface (FS) warping as in Sr_2RuO_4 (Ref. 20) (the magnitude only increases by 1% with an increase of 1 T, compared to an increase of 8% in ρ_{ab}). In the mixed phase an *additional* fourfold symmetry develops with minima located along [110] and [1$\bar{1}$0], offset 45° from the minima observed in ρ_{ab} in the FFM phase. From the mixed phase to the FFM phase this anisotropy evolves smoothly. This anisotropy can be attributed to spin polarization of the $d_{xz,yz}$ orbitals as discussed

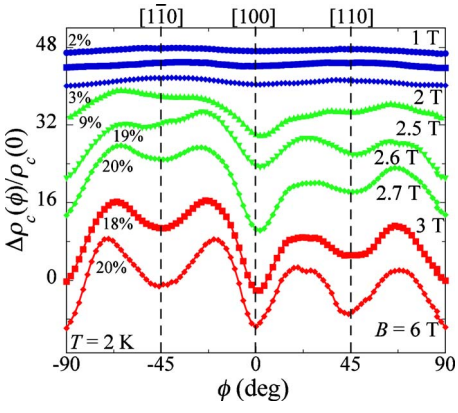

FIG. 3. (Color online) Normalized azimuthal angle dependence of c-axis magnetoresistivity $\Delta\rho_c(\phi)/\rho_c(0)$ at selected applied magnetic fields and 2 K. From the top down: 1.0, 1.5, and 2.0 T are within the LP phase, 2.5, 2.6, and 2.7 T are within the mixed phase, and 3.0 and 6.0 T are within the FFM phase. The relative magnitude of anisotropy is indicated in percentage.

below. We have also measured field sweeps of ρ_c at various θ [see Fig. 2(c)] and ϕ, respectively, from which the anisotropy due to misalignment is estimated to be $<0.1\%$ in the LP and FFM phases, nearly negligible compared to the observed AMR (3% for LP and 20% for FFM), and $\sim 20\%$ in the mixed phase, which is comparable to the observed AMR ($\sim 8-20$ %), giving rise to a clear asymmetry.

The observation of extraordinarily different anisotropic properties in ρ_{ab} and ρ_c suggests that the metamagnetism in $Sr_4Ru_3O_{10}$ is orbital dependent. Below we discuss the origin of each unique type of anisotropy observed. As indicated above, the ρ_{ab} anisotropy in the LP phase has symmetry of the form $A+D\sin^2(\phi)$ [Fig. 1(c)]. This symmetry is consistent with magnetocrystalline anisotropy theoretically predicted and experimentally observed in 3*d* FM metals or 4*d* FM metal $SrRuO_3$, with spin-orbit coupling.[21–23] Spin-orbit coupling competes with crystal-field splitting to create preferential spin orientations, causing anisotropy in magnetoresistivity. In the LP phase, FM domain-wall scattering should play a minor role in magnetotransport since typical domain-wall scattering dominated transport properties, i.e., negative magnetoresistance,[24] were not observed here [see Figs. 2(b) and 2(c)]. The strong field dependence of the magnitude of anisotropy is also consistent with expectations for Ising-type FM anisotropy.

In the mixed phase the presence of FFM domains results in spin scattering between LP and FFM domains. The spin scattering increases initially with the growth of FFM domains, but decreases when FFM domains become large enough so that they can become connected, eventually diminishing as FFM domains form a percolative network.[13] We can attribute the large anisotropy of magnetoresistivity of the mixed phase to field-orientation-dependent spin scattering. When applied field is well below the field for the formation of percolation and oriented along the easy axis [100] the FFM domains are larger, increasing the spin scattering rate and resistivity, whereas with field along the hard axis, FFM domains are smaller, causing a lesser spin scattering rate and smaller resistivity. The local minima located within the [100] maxima is due to the presence of LP domains in the mixed phase.

Previous Raman spectroscopy studies revealed that the metamagnetic transition is accompanied by enhanced spin-phonon coupling,[16] suggesting the transition involves a change in the lattice degree of freedom. Moreover, thermopower shows an unusual increase across the transition as noted above, which points to a change in the orbital degree of freedom.[18] These implications suggest that the FM anisotropy caused by spin-orbit coupling may change with the metamagnetic transition. The transition from twofold symmetry below B_c to fourfold symmetry above B_c, indicates that the lattice and orbital degrees of freedom have changed in such a way that spin polarization becomes equivalent between [100] and [010], resulting in an anisotropy with a symmetry consistent with the electron density expected for a d_{xy} orbital.

ρ_c anisotropy exhibits markedly different symmetry than ρ_{ab}, as described above. In the LP phase the fourfold anisotropy with minima along [100] and [010] is non-FM type since it is inconsistent with the twofold anisotropy observed

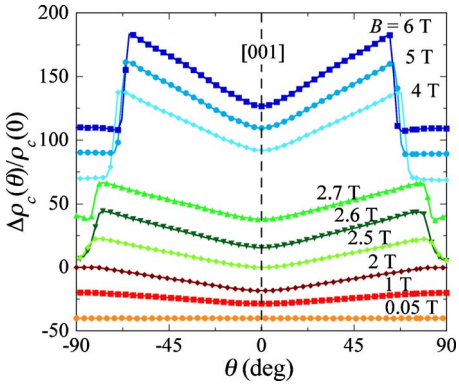

FIG. 4. (Color online) Polar angle dependence of normalized *c*-axis magnetoresistivity $\Delta\rho_c(\theta)/\rho_c(0)$ at selected applied magnetic fields and 2 K. When fields are oriented in the *ab* plane (θ=90°), from the bottom up: 0.05, 1.0, and 2.0 T are within the LP phase, 2.5, 2.6, and 2.7 T are within the mixed phase, and 4.0, 5.0, and 6.0 T are within the FFM phase.

in ρ_{ab} and has a weak field dependence, indicating that ρ_c does not exhibit a FM response. Instead this anisotropy can be attributed to Fermi-surface warping, as mentioned above.[20] Above B_c in the FFM phase ρ_c exhibits an *additional* fourfold anisotropy with minima along $[110]/[1\bar{1}0]$, offset by 45° from the ρ_{ab} minima. We have already established that the ρ_{ab} FFM phase anisotropy is consistent with d_{xy} orbital symmetry, so taking into account the 45° offset we can see that this additional ρ_c anisotropy is consistent with the symmetry of the $d_{xz,yz}$ orbitals. In light of this symmetry consistency with the $d_{xz,yz}$ and that spin polarization is a requirement for magnetic anisotropy our observation of ρ_c anisotropy in the FFM phase suggests that the $d_{xz,yz}$ orbitals are unpolarized below B_c and only become FM in nature above the metamagnetic transition. The polarization of the $d_{xz,yz}$ orbitals only above B_c is further evidenced in polar angle dependence of $\rho_c(B)$ shown in Fig. 4. When $B<B_c$, ρ_c gradually increases with increasing angle, but with no clear anomaly. When $B>B_c$, a sharp drop in ρ_c develops for polar angles close to the *ab* plane, resulting in a higher conductivity state, indicating a transition to a polarized state.

The orbital dependence of magnetism in $Sr_4Ru_3O_{10}$ can be ascribed to FS peculiarities caused by RuO_6 octahedron rotation. The effect of RuO_6 rotation on the FS has been examined in single-layered $Ca_{2-x}Sr_xRuO_4$,[25] which revealed that RuO_6 rotation caused by partial Ca substitution for Sr ($0.5\leq x\leq 2.0$) results in a downward shift of the Ru $4d_{xy}$ band, moving the Van Hove singularity (VHS) closer to the Fermi level (FL). Octahedron rotation in $Sr_3Ru_2O_7$ appears to have a similar effect. Recent photoemission spectroscopy studies on $Sr_3Ru_2O_7$ revealed that the γ_2 FS pocket, derived from the d_{xy} orbital, indeed has a VHS slightly below the FL, which is favorable for magnetic instability.[26] Since the octahedra rotation in the central layer of each triple layer in $Sr_4Ru_3O_{10}$ is greater than the rotation in $Sr_3Ru_2O_7$,[11] it can be extrapolated that the VHS should be closer to or at the FL in $Sr_4Ru_3O_{10}$. As a result, the ferromagnetism seen in the LP phase can be attributed to the VHS in the density of states at the FL in the d_{xy} bands, whereas the bands from $d_{xz,yz}$ orbitals are not polarized until $B\geq B_c$.

This orbital-selective metamagnetic transition scenario is consistent with the early result of high magnetic field measurements on $Sr_4Ru_3O_{10}$.[27] That experiment revealed that when magnetic field is rotated out of the plane, the metamagnetic transition bifurcates into two separate transitions. The one occurring at low fields shows behaviors consistent with a FM state. The other which moves to higher field with larger out-of-plane angles, shows characteristics consistent with an itinerant metamagnetic transition. The enhancement of the ρ_c minima along [100] and [010] above B_c (Fig. 3) should be associated with the change in FS across the transition.

The role of the orbital degree of freedom in governing the magnetism of $Sr_4Ru_3O_{10}$ provides us with insights into complex magnetic properties of other ruthenates, such as competing magnetic fluctuations in $Sr_3Ru_2O_7$ (Ref. 28) and multiple magnetic phase transitions in $(Sr_{1-x}Ca_x)_3Ru_2O_7$, which includes itinerant metamagnetic, nearly FM, and AFM states.[29] The orbital degree of freedom may be active in all of these materials. Similar studies on these materials may reveal their underlying orbital physics.

In summary, we investigated the anisotropic properties of magnetoresistivity for various magnetic states in $Sr_4Ru_3O_{10}$. Our results suggest that the metamagnetic transition in $Sr_4Ru_3O_{10}$ is orbital selective. The ρ_{ab} anisotropy with twofold Ising-type symmetry below the metamagnetic transition indicates that the d_{xy} orbital is ferromagnetic in the ground state, whereas the fourfold ρ_c anisotropy below the transition originates from Fermi-surface warping. Only above the transition does ρ_c exhibit ferromagnetic anisotropy, suggesting that the metamagnetic transition in $Sr_4Ru_3O_{10}$ originates from the $d_{xz,yz}$ orbitals.

Work at Tulane is supported by DOE under Grant No. DE-FG02-07ER46358 (personnel support), NSF under Grant No. DMR-0645305 (support for equipment), the DOD ARO under Grant No. W911NF0910530 (support for materials), and the Research Corporation.

*zmao@tulane.edu

[1] H. Kawano, H. Yoshizawa, and Y. Ueda, J. Phys. Soc. Jpn. **63**, 2857 (1994).
[2] M. Noguchi, A. Nakazawa, S. Oka, T. Arima, Y. Wakabayashi, H. Nakao, and Y. Murakami, Phys. Rev. B **62**, R9271 (2000).
[3] Y. Tokura and N. Nagaosa, Science **288**, 462 (2000).
[4] B. Keimer, Nat. Mater. **5**, 933 (2006).
[5] M. Kubota, Y. Murakami, M. Mizumaki, H. Ohsumi, N. Ikeda, S. Nakatsuji, H. Fukazawa, and Y. Maeno, Phys. Rev. Lett. **95**, 026401 (2005).
[6] I. Zegkinoglou *et al.*, Phys. Rev. Lett. **95**, 136401 (2005).
[7] V. I. Anisimov, I. A. Nekrasov, D. E. Kondakov, T. M. Rice, and M. Sigrist, Eur. Phys. J. B **25**, 191 (2002).
[8] S. Wang and H. Ding, New J. Phys. **7**, 112 (2005).
[9] D. F. Agterberg, T. M. Rice, and M. Sigrist, Phys. Rev. Lett. **78**, 3374 (1997).
[10] K. Deguchi, Z. Mao, and Y. Maeno, J. Phys. Soc. Jpn. **73**, 1313 (2004).
[11] M. K. Crawford, R. L. Harlow, W. Marshall, Z. Li, G. Cao, R. L. Lindstrom, Q. Huang, and J. W. Lynn, Phys. Rev. B **65**, 214412 (2002).
[12] G. Cao, L. Balicas, W. H. Song, Y. P. Sun, Y. Xin, V. A. Bondarenko, J. W. Brill, S. Parkin, and X. N. Lin, Phys. Rev. B **68**, 174409 (2003).
[13] Z. Q. Mao, M. Zhou, J. Hooper, V. Golub, and C. J. O'Connor, Phys. Rev. Lett. **96**, 077205 (2006).
[14] D. Fobes, M. H. Yu, M. Zhou, J. Hooper, C. J. O'Connor, M. Rosario, and Z. Q. Mao, Phys. Rev. B **75**, 094429 (2007).
[15] Y. Nakajima, Y. Matsumoto, D. Fobes, M. Zhou, Z. Q. Mao, and T. Tamegai, J. Phys.: Conf. Ser. **150**, 042134 (2009).
[16] R. Gupta, M. Kim, H. Barath, S. L. Cooper, and G. Cao, Phys. Rev. Lett. **96**, 067004 (2006).
[17] G. Cao, S. Chikara, J. W. Brill, and P. Schlottmann, Phys. Rev. B **75**, 024429 (2007).
[18] Z. Xu, X. Xu, R. S. Freitas, Z. Long, M. Zhou, D. Fobes, M. Fang, P. Schiffer, Z. Mao, and Y. Liu, Phys. Rev. B **76**, 094405 (2007).
[19] M. Zhou, J. Hooper, D. Fobes, Z. Mao, V. Golub, and C. O'Connor, Mater. Res. Bull. **40**, 942 (2005).
[20] E. Ohmichi, Y. Maeno, S. Nagai, Z. Q. Mao, M. A. Tanatar, and T. Ishiguro, Phys. Rev. B **61**, 7101 (2000).
[21] J. Eckstein, I. Bozovic, J. O'Donnell, M. Onellion, and M. Rzchowski, Appl. Phys. Lett. **69**, 1312 (1996).
[22] W. Limmer, M. Glunk, J. Daeubler, T. Hummel, W. Schoch, R. Sauer, C. Bihler, H. Huebl, M. S. Brandt, and S. T. B. Goennenwein, Phys. Rev. B **74**, 205205 (2006).
[23] O. Morán, W. Saldarriaga, and E. Baca, Solid State Sci. **11**, 1187 (2009).
[24] D. Ravelosona, A. Cebollada, F. Briones, C. Diaz-Paniagua, M. A. Hidalgo, and F. Batallan, Phys. Rev. B **59**, 4322 (1999).
[25] Z. Fang and K. Terakura, Phys. Rev. B **64**, 020509(R) (2001).
[26] A. Tamai *et al.*, Phys. Rev. Lett. **101**, 026407 (2008).
[27] Y. J. Jo, L. Balicas, N. Kikugawa, E. S. Choi, K. Storr, M. Zhou, and Z. Q. Mao, Phys. Rev. B **75**, 094413 (2007).
[28] L. Capogna, E. M. Forgan, S. M. Hayden, A. Wildes, J. A. Duffy, A. P. Mackenzie, R. S. Perry, S. Ikeda, Y. Maeno, and S. P. Brown, Phys. Rev. B **67**, 012504 (2003).
[29] Z. Qu *et al.*, Phys. Rev. B **78**, 180407(R) (2008).